INSTITUTE OF PHYSICS PUBLISHING NANOTECHNOLOGY
Nanotechnology **17** (2006) 2032–2039 doi:10.1088/0957-4484/17/8/041

# Biochemical functionalization of vertically aligned carbon nanofibres

**Benjamin L Fletcher**[1], **Timothy E McKnight**[2], **Anatoli V Melechko**[1], **Michael L Simpson**[1,3] **and Mitchel J Doktycz**[3,4]

[1] University of Tennessee, Knoxville, TN 37996, USA
[2] Engineering Science and Technology Division, Oak Ridge National Laboratory, PO Box 2008, MS 6123, Oak Ridge, TN 37831, USA
[3] Condensed Matter Sciences Division, Oak Ridge National Laboratory, PO Box 2008, MS 6123, Oak Ridge, TN 37831, USA
[4] Life Sciences Division, Oak Ridge National Laboratory, PO Box 2008, MS 6123, Oak Ridge, TN 37831, USA

E-mail: doktyczmj@ornl.gov

Received 16 August 2005, in final form 14 December 2005
Published 24 March 2006
Online at stacks.iop.org/Nano/17/2032

**Abstract**
Because of their unique physical and chemical properties, vertically aligned carbon nanofibres (VACNFs) show promise in improving current analytical measurement techniques. Chemical functionalization schemes will be necessary to fully realize this promise. Functionalization of the VACNFs with biomolecules or other species can impart specific chemical or physical properties. We report on two methods for immobilizing biomolecules on the surface of VACNFs. One attachment scheme makes use of a class of heterocyclic aromatic dye compounds to specifically adsorb onto VACNFs. The second scheme involves covalently coupling biomolecules through cross-linking to carboxylic acid sites on the sidewalls of the carbon nanofibres. The observed adsorption and covalent coupling properties are consistent with the physical structure and chemical characteristics of the VACNFs.

## 1. Introduction

Nanoscale materials promise to improve analytical measurement techniques. They allow for a high degree of miniaturization and present unique physical properties that augment the functionality of physical devices. For example, the small size of nanostructures enables potential routes for interfacing and controlling biological systems. Vertically aligned carbon nanofibres (VACNFs) are one such material. The ability to control the synthesis of these structures and to direct their assembly over wafer scale dimensions is enabling applications in chemical sensing [1, 2], in biological interfacing [3, 4], and in mimicry of biological structures [5]. Carbon nanofibres, with tip diameters as small as 10 nm and lengths up to several tens of microns, can be grown from catalytic metal particles by a plasma enhanced chemical vapour deposition process [6]. Growth of individual and multiple vertically aligned carbon nanofibres can be directed by traditional lithographic methods allowing for accurate positioning of carbon nanofibres across spatial dimensions ranging from nanometres to centimetres [7]. Further, manipulation of the growth process can be used to control the length, shape, and vertical alignment of the nanofibres [8, 9]. This control over synthesis at the nanoscale can be combined with conventional micromachining techniques for both top-down and bottom-up fabrication of complex structures. The ability to create structures on multiple length scales is a requirement for relaying nanoscale phenomena through conventional scale interfaces.

To realize functional devices employing carbon nanostructures, specific chemical attachment schemes are often required. Derivatization of the VACNFs with biomolecules or other species will be necessary for imparting specific chemical or physical properties to the VACNFs. Derivatization schemes for VACNFs depend on coupling to the outer layer of graphene sheets. A related structure is found in single walled carbon nanotubes (CNTs) and several derivatization schemes have been

 © 2006 IOP Publishing Ltd Printed in the UK 

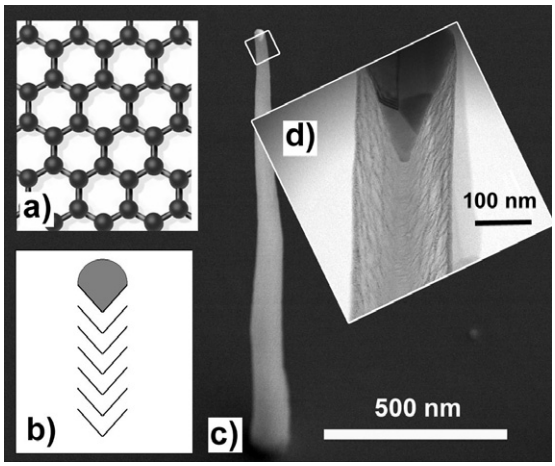


**Figure 1.** Details of the carbon nanofibre structure. Planar sheets of graphene (a) are formed during the growth process and are structured in a stacked funnel-like configuration (b). Such structures can be observed from analyses of single vertically aligned carbon nanofibres (c) and high-resolution TEM images (d). This morphology provides high numbers of defect sites at the surface of VACNFs.

described. These approaches exploit the presence of carboxylic acid functionalities at either the uncapped ends or at defect sites along nanotube sidewalls or, alternatively, use chemistries that directly attach to the graphene surface [10–14]. Adsorption strategies have also been exploited. Examples in this latter category include the adsorption of pyrene, proteins, and complex polymers [15–18]. In contrast to CNTs, VACNFs are composed of multiple layers of graphene (figure 1(a)) that appear 'bamboo'-like or as 'stacked funnels' (figure 1(b)) when viewed from the side using the transmission electron microscope (TEM). The graphene edges terminate on the sidewalls (figure 1(b) of the VACNF (figure 1(c)) as can be seen in a TEM image (figure 1(d)). Under specific growth conditions, the graphene edges of VACNFs can be terminated by hydrogen. For such nanofibres, Baker *et al* have demonstrated that these hydrogen terminated edges can be functionalized either via a photochemical reaction with molecules bearing an alkene moiety or via reaction with a diazonium salt [19], thereby effectively providing more convenient handles for subsequent biochemical functionalization such as carboxylic acid or primary amine groups. Under some growth conditions, these moieties are already present upon as-synthesized fibres, and can be exploited without additional derivatization procedures. Under different growth parameters, other surface conditions can result upon the nanofibres including amorphous carbon films and/or materials sputtered from the substrate and deposited upon the nanofibre sidewalls during nanofibre synthesis. The wide variation in surface properties of as-synthesized nanofibres thereby requires a variety of functionalization schemes for both characterizing the nanofibre surface and immobilizing desired species upon it.

Here we investigate several approaches for both characterizing and functionalizing, i.e. immobilizing biomolecules to, as-synthesized VACNFs. One approach is based on the specific adsorption of a class of heterocyclic aromatic compounds typically used for the fluorescent labelling of biomolecules. This interaction enables a facile approach to coupling biomolecules to the sidewalls of the carbon nanofibres as well as a convenient fluorescent labelling method for visualization and assessment of the reaction. A second approach involves covalent coupling of biomolecules to carboxylic acid sites present on the sidewalls of as-synthesized carbon nanofibres. This method of attachment leads to a stable, covalent linkage. Both approaches are used for adding chemical specificity to VACNFs as demonstrated by the specific capture of selected protein and DNA molecules.

## 2. Methods and materials

### *2.1. Materials*

Tetramethylrhodamine, rhodamine-B base, fluorescein, avidin, fluorescein–biotin, rhodamine–streptavidin, fluorescein–streptavidin, tetramethylrhodamine–avidin, 1-ethyl-3-(3-dimethylaminopropyl) carbodiimide (EDC), and morpholinoethanesulfonic acid (MES) were obtained from Sigma-Aldrich (St Louis, MO). Synthetic DNA oligonucleotides were purchased from Integrated DNA Technologies (Coralville, IA). Silicon wafers were obtained from Silicon Quest International (Santa Clara, CA). Proteins were selected due to their commercial availability. All materials were used as received from the manufacturer.

### *2.2. Structure preparation*

VACNFs were prepared from nickel catalyst thin films that were deposited by evaporation and patterned on a Si wafer substrate by photolithography. For examining chemical coupling schemes, existing photomasks were used. These patterns were arbitrarily selected, but are currently used for creating nanofibre-based membranes in microfluidic structures or for generating arrays of nanofibres appropriate for cellular penetration and interfacing. Both of these applications will benefit from the chemical functionalization of VACNFs. An example structure is shown in figure 2. This structure consists of a microfluidic channel that was etched in a silicon substrate using a reactive ion etcher. Nickel catalyst was deposited and patterned via lift-off on the channel floor for subsequent growth of VACNFs. VACNF growth was performed using a previously defined plasma-enhanced chemical vapour deposition (PECVD) process (see [6] and references therein). Briefly, the wafer was maintained at 700 °C, while a mixture of $C_2H_2$ and $NH_3$ was introduced into the PECVD chamber at 3 Torr of pressure. Plasma was initiated and maintained at 450 V and 300 mA. Growth of individual nanofibres resulted primarily from the catalytic deposition of carbon through the nickel particle at the growing nanofibre tip with the additional deposition of carbonaceous material on the nanofibre surface. Ammonia serves as an etchant to remove a passivating carbon film that continuously forms on the surface of the catalyst particle and nanofibre sidewalls. Variations in the acetylene/ammonia ratio allow for substantial control over the chemical composition of the carbon nanofibre sidewall coating, i.e. carbon [20] at high values of this ratio or silicon carbonitride at very low values [21]. Also, the $C_2H_2$ flow rate may be adjusted to effectively grow the carbon nanofibres in different spatial patterns. For the structures presented in figures 2 and 3 the $C_2H_2$ flow rates were 60 and

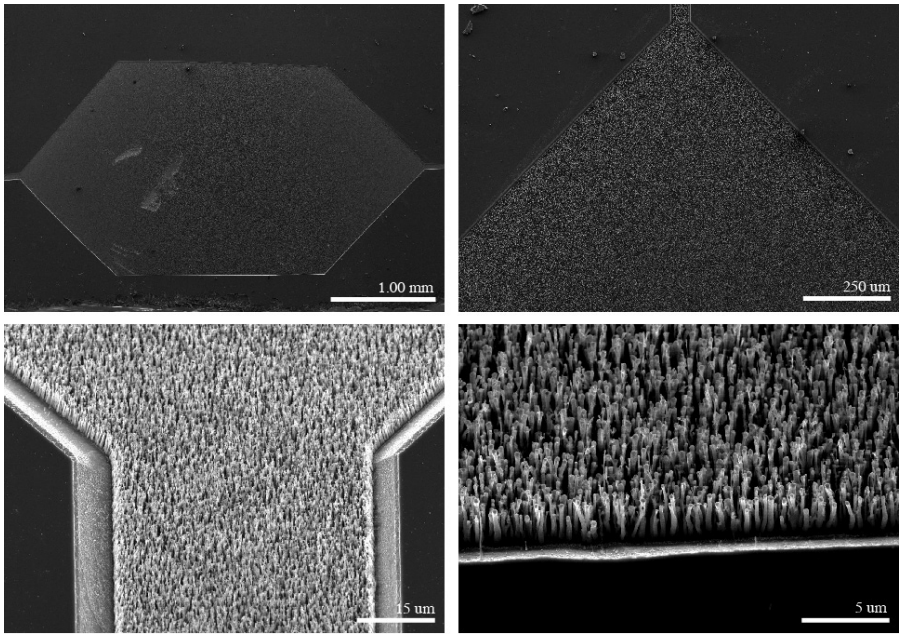


**Figure 2.** Electron micrographs of a typical VACNF structure used in characterization experiments. A microfluidic channel was etched into the silicon substrate and a carbon nanofibre forest was grown from nickel deposited on the channel floor.

55 sccm, respectively, and the $NH_3$ flow rate was maintained at 80 sccm. The structure and composition was verified by electron microscopies (SEM, STEM, TEM) and spectroscopies (EDX and Auger) and was determined to be the same for all the nanofibres used in the experiments described here. The positions of individual nanofibres within a region of catalyst are random, though the physical characteristics of individual nanofibres are similar. The nanofibres are typically $\sim$10 $\mu$m tall and $\sim$400 nm wide at the base, tapering to $\sim$100 nm at the tip. Following nanofibre growth, the wafers were cleaved into 1 cm $\times$ 1 cm chips containing arrays of VACNFs.

### *2.3. Adsorption—small molecules*

The three dyes examined for adsorption studies included tetramethylrhodamine, rhodamine-B base, and fluorescein. A 10 mg $\mu$l$^{-1}$ stock solution of each was prepared by dissolving the appropriate amount in deionized water. The dyes were further diluted in deionized water at a 1:10 ratio. Higher concentrations did not lead to changes in the experimental results. For a typical experiment a small amount of the diluted dye solution ($\sim$5 $\mu$l) was dispensed onto a VACNF array using a pipette. After allowing for adsorption to occur for $\sim$10 min, the structure was washed using deionized water from a squirt bottle for $\sim$1 min and dried with a stream of air. Longer wash times had no effect on measured signals. Samples prepared with longer adsorption times showed no noticeable improvement.

### *2.4. Absorption—proteins*

Avidin, tetramethylrhodamine–avidin, rhodamine–streptavidin, and fluorescein–streptavidin were prepared as 5 mg ml$^{-1}$ solutions and were selected due to their commercial availability. These protein reagents were diluted in phosphate-buffered saline (PBS: 10 mM sodium phosphate, 150 mM NaCl, pH 7.4) in a 1:10 ratio. For these experiments, a small amount ($\sim$5 $\mu$l) was dispensed onto a VACNF array and left for $\sim$10 min. The structure was then washed using deionized water from a squirt bottle for $\sim$1 min and dried with a stream of air.

To assess the chemical activity of protein functionalized VACNFs, streptavidin or avidin conjugated nanofibres were prepared as described above and reacted with fluorescein–biotin. The fluorescein–biotin was prepared in 2.5 mg ml$^{-1}$ stock solutions and was further diluted in PBS at a 1:10 ratio. A small ($\sim$5 $\mu$l) amount was spotted onto the nanofibres, the reaction was allowed to occur for $\sim$10 min and the structure was washed using deionized water from a squirt bottle for $\sim$1 min and dried with a stream of air.

### *2.5. Covalent cross-linking*

Before chemical treatment, VACNFs were exposed to an oxygen plasma for 30 s to promote the abundance of carboxylic acid groups. VACNF structures were then immersed in a 100 mM solution of MES at pH 4.9. A 10 mg ml$^{-1}$ solution of EDC and 10 $\mu$l of reactant were added to the MES buffer. Coupling was allowed to occur for 24 h. The VACNF structures were then immersed in a 4 M urea solution (pH 9.2) and vortexed for $\sim$5 min. This chaotropic wash removed the reactant that was non-specifically bound to the VACNF structures. Avidin, fluorescein–streptavidin, and a synthetic DNA oligonucleotide containing a 5′ alkyl amine functionalization were tethered to carbon nanofibres using this method. The VACNF structures cross-linked with avidin were spotted with a small amount ($\sim$5 $\mu$l) of fluorescein–biotin and left to incubate for $\sim$10 min. The VACNF structures that were cross-linked with DNA (18 nucleotide sequence complementary to the T7 promoter) were hybridized with a small amount ($\sim$15 $\mu$l) of oligonucleotide. The oligonucleotide was either complimentary or uncomplimentary

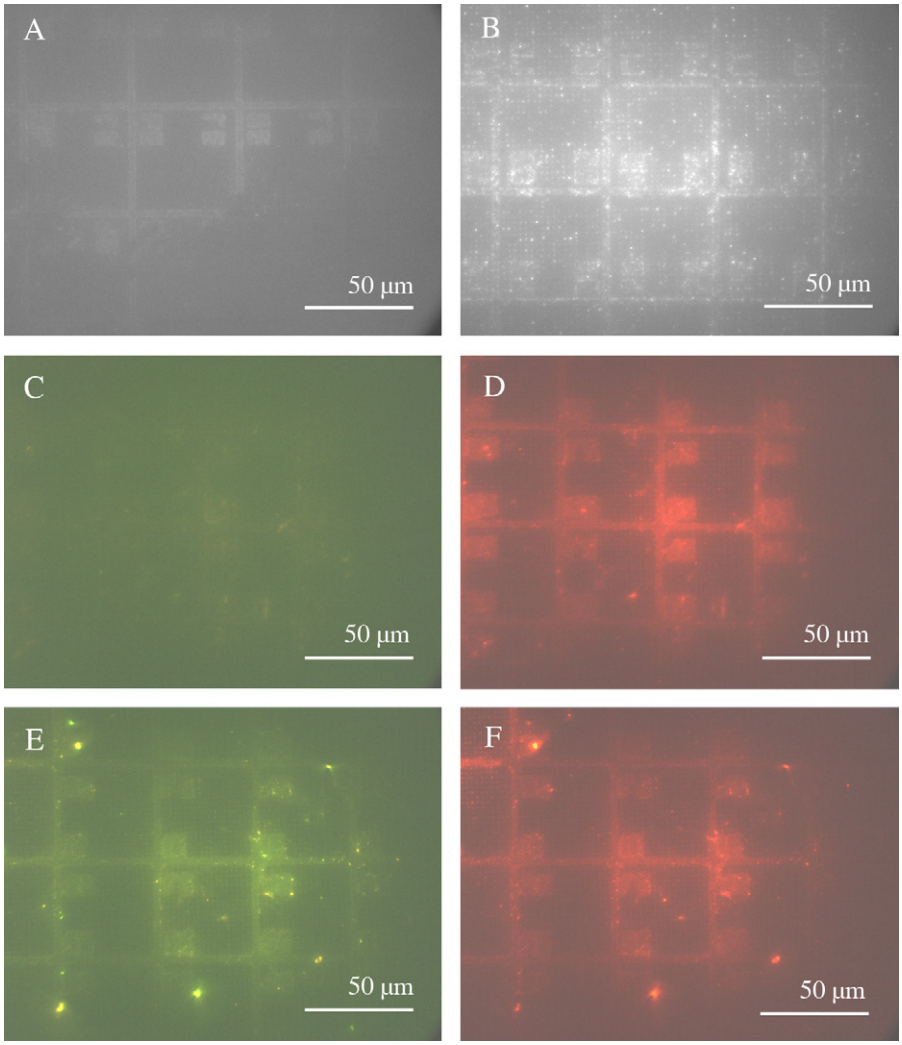


**Figure 3.** Fluorescence micrographs of carbon nanofibre arrays. At the top, fluorescein (A) or tetramethylrhodamine (B) dyes were spotted onto an array of carbon nanofibres, allowed to adsorb, and then washed and imaged using the appropriate filter set. The carbon nanofibre array consists of individual nanofibres spatially indexed within an alphanumerically labelled grid of carbon nanofibres. The tetramethylrhodamine specifically attaches to the carbon nanofibres while fluorescein does not. Contrast between individual VACNFs and the background substrate can be readily discerned for adsorbed tetramethylrhodamine. In (C) and (D), rhodamine–streptavidin was adsorbed to the carbon nanofibres and then reacted with fluorescein–biotin ((E) and (F)). Images (C) and (E) were taken using a fluorescein filter set while images (D) and (F) were collected using a rhodamine filter set.

and end labelled with CY3. These probes were prepared in PBS at a concentration of 1 $\mu$M. After reaction, the structures were immersed in a 400 mM NaCl solution and vortexed for ∼5 min to remove non-specifically bound reactant from the VACNFs and substrate. A brief (∼5 s) rinse with a deionized water spray bottle washed off the remaining NaCl solution. The structure was blow dried with air and imaged to assess the reaction.

### *2.6. Characterization*

A high-resolution cold cathode field emission scanning electron microscope (Hitachi S4700) was used for analysis of the prepared VACNF arrays. The accelerating voltage for SEM imaging was optimized at 10 kV. Images were acquired with the beam incident normal to the surface or at a 30° tilt. For analysis of fluorescently labelled VACNFs, an epi-fluorescence microscope (Zeiss Axioscop 2FS) using long pass emission rhodamine and fluorescein filter sets and equipped with a Retiga EX CCD camera was used. Alternatively, a Leica SP2 confocal microscope was employed.

## 3. Results

### *3.1. Absorption based functionalization of carbon nanofibres*

To assess the specificity and usefulness of adsorption as a mechanism for chemical functionalization, standard proteins and a set of conventional fluorescent organic dyes were used. This latter set included fluorescein, tetramethylrhodamine, and rhodamine-B base. The structure was simply wetted with a solution of the dye to assess adsorption. For fluorescein, washing with deionized water proved sufficient to remove all traces of the dye from the nanofibre surface as judged by fluorescence microscopy. No detectable fluorescence was

observed using image integration times of 300 ms. Integration times were chosen as the time at which the background fluorescence of unmodified carbon nanofibres was barely measurable. A typical result is shown in figure 3(A). A small amount of autofluorescence from the nanofibres produces some background fluorescence. However, rhodamine-B base and tetramethylrhodamine coupled strongly enough to withstand vigorous (∼1 min) washes in deionized water and salt solutions (400 mM NaCl). As shown in figure 3(B), the tetramethylrhodamine dye adheres to the carbon nanofibres as judged by the fluorescence collected using a rhodamine filter set. Similar results were observed with rhodamine-B base (results not shown). It should be noted that a fraction of experiments involving rhodamine dyes showed a weak or negligible adsorption interaction. Brief washes (∼1 min) with deionized water were sufficient to remove some of the adsorbed rhodamine dye. This phenomenon was attributed to contamination of the carbon nanofibre surface in these specific cases. An oxygen plasma cleaning, prior to experimentation, improved adsorption to the VACNF structures. It was determined that fluorescein failed to interact with the nanofibres under any conditions, as fluorescence was never detected above background using the standard exposure time.

To demonstrate protein functionalization by an adsorption-based strategy, avidin or streptavidin conjugated with fluorescent dyes were reacted with VACNF arrays. The reagents examined included fluorescein–streptavidin, rhodamine-streptavidin, and tetramethylrhodamine–avidin. Fluorescein conjugated streptavidin showed no interaction with the VACNFs, as no fluorescence was detected. For similar image integration times, VACNFs reacted with rhodamine dyes conjugated to avidin or streptavidin showed fluorescence, indicating adsorption. The fluorescent labelling of the VACNFs using rhodamine–streptavidin is seen in figure 3(C) (fluorescein filter set) and 3D (rhodamine filter set). Similar results were observed when using tetramethylrhodamine labelled avidin. These adsorption results are consistent with the results obtained using unconjugated dyes. Further, pretreatment of the carbon nanofibres with unconjugated avidin for 10 min did not prevent binding of the dye conjugated protein. This indicates that avidin itself has negligible affinity for the nanofibre surface. This is significant as it indicates that the specific association is due to the attached rhodamine dyes. Fluorescein–biotin, for which avidin and streptavidin have a high specific affinity, also showed no interaction with the carbon nanofibres. However, adsorbed rhodamine–streptavidin retains some biotin affinity, as indicated by the ability to bind added fluorescein-labelled biotin. This is shown in figures 3(E) and (F) where fluorescently labelled VACNFs are observed when using both fluorescein and rhodamine filter sets. The capture of fluorescein–biotin in figure 3(E) can be assessed by comparison with figure 3(C), which shows the lack of signal in the fluorescein channel before the reaction. Vortexing the structures in deionized water or PBS for 5 min was insufficient to break the bond formed between the rhodamine dye and carbon nanofibre surface as well as the bond formed between streptavidin and biotin. However, immersing the VACNF structures in 4 M urea and vortexing for 5 min removed all detectable traces of adsorbed protein-conjugated dyes.

### *3.2. Covalent coupling to carbon nanofibres*

Covalent coupling through a diimide activated amidization between the carboxylic acid groups on the surface of carbon nanofibres and primary amine groups on proteins was also assessed. Figure 4(A) shows that, while fluorescein-conjugated streptavidin does not adsorb to VACNFs, it is possible to covalently attach it. Fluorescein conjugated streptavidin remains attached to the VACNFs even after washing with a chaotropic reagent, such as 4 M urea (right-hand image in figure 4(A)). This wash is sufficient to remove adsorbed material. Figures 4(B) and (C) display the fluorescent micrographs collected using fluorescein and rhodamine filter sets, respectively, when rhodamine conjugated streptavidin was covalently coupled to the VACNFs and washed with 4 M urea (centre panels). Integration times for the images collected under both the fluorescein and rhodamine filter sets was 300 ms. After reacting with fluorescein–biotin and washing with 400 mM NaCl to remove non-specifically bound material (right-hand panels), fluorescence is observed using both filter sets. Figures 4(B) and (C) show that after covalent attachment the biotin affinity of attached proteins is retained. Avidin, without conjugated dyes, can also be covalently cross-linked to carbon nanofibres and still bind with fluorescein-conjugated biotin (not shown).

In order to achieve initial protein modification of the nanofibre using this method, a sufficient number of carboxylic acid sites must be formed on the VACNF's surface for covalent attachment. Oxygen plasma cleaning promoted carboxylic acid formation. Structures were immersed in 4 M urea solutions and vortexed for 5 min to remove any contaminants. These washes also removed background fluorescence and did not adversely affect the covalently tethered protein and conjugated biotin.

Covalent coupling was also used to tether a DNA probe to the surface of the VACNFs. An 18 base oligonucleotide was functionalized with an alkyl amine on the 5′ end to enable amidization with the VACNF structure in the presence of EDC. Hybridization with a complementary CY3 labelled oligonucleotide with the immobilized DNA is shown in figure 5. Examination of the structure with captured fluorescently labelled DNA by confocal fluorescence microscopy shows that the DNA is captured along the entire length of the VACNFs. The VACNFs in this image are ∼4 $\mu$m tall as measured using a scanning electron microscope. Exposure of either a DNA functionalized structure or a non-functionalized structure with a fluorescently labelled, non-complementary sequence showed no labelling.

## 4. Discussion

Chemical functionalization protocols are often a necessary first step for numerous applications including chemical and biochemical sensing applications. Such procedures add chemical specificity that is not intrinsic to the parent material. Understanding non-specific interactions with nanomaterials is equally important, especially for sensing applications, because such interactions can lead to background signals or fouling of the material. Further, understanding non-covalent interactions can provide insight into the chemical nature of the

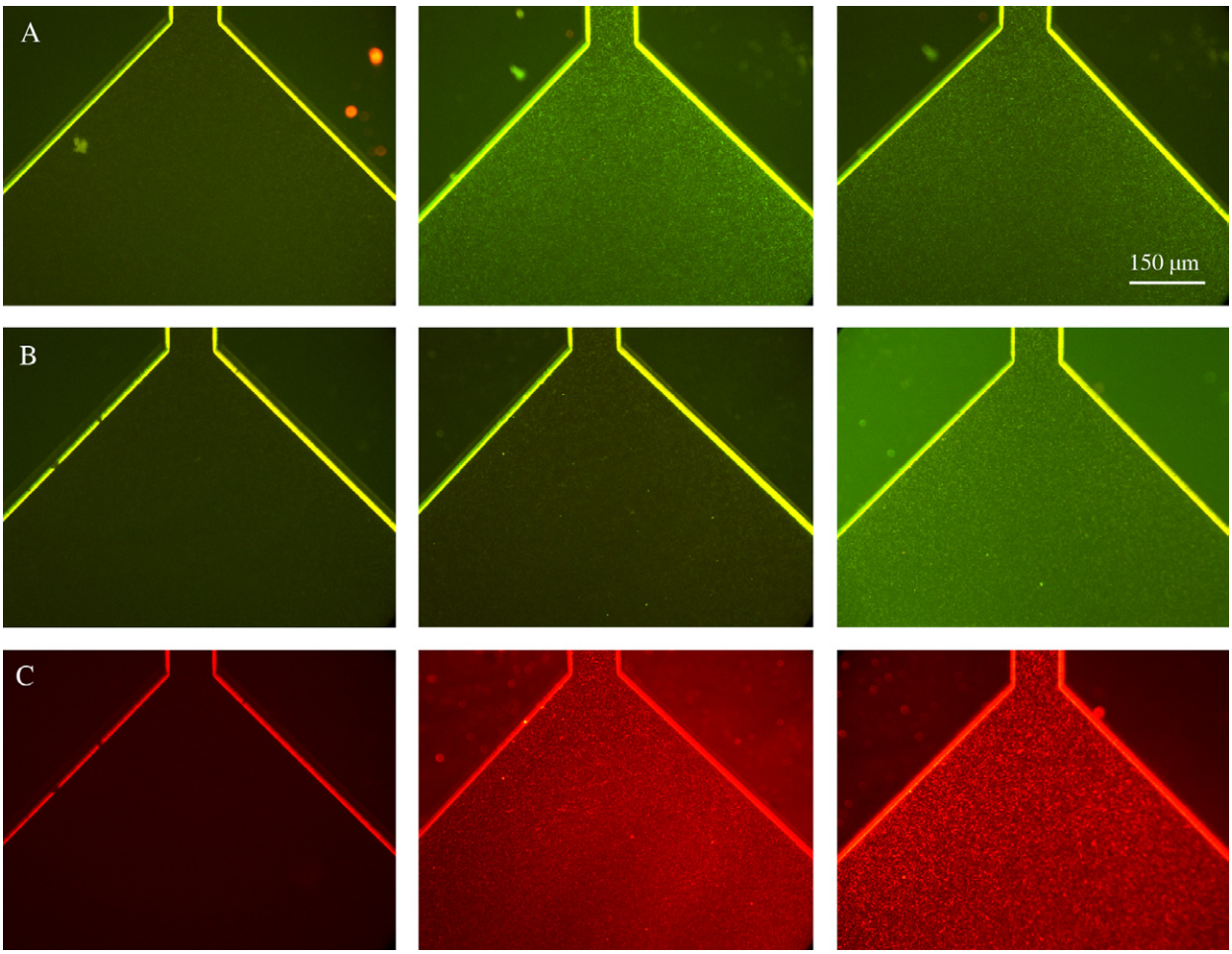


**Figure 4.** Fluorescence micrographs of a forest of carbon nanofibres. The VACNFs are patterned within a microfluidic channel that can be readily discerned due to the refracted light that reaches the detector. The surrounding area does not contain VACNFs and serves as a reference for background signal that may originate from non-specific binding to the substrate. In (A), the image on the left displays the structure before tethering fluorescein–streptavidin to the carbon nanofibres, the centre image shows the structure after coupling the conjugated protein using EDC, while the image on the right displays the structure after washing with 4 M urea. In (B) and (C), rhodamine–streptavidin was tethered to the carbon nanofibres using EDC and washed with 4 M urea (middle) then reacted with fluorescein–biotin and washed with 400 mM NaCl (right). The structure prior to any treatment is shown on the left. The images shown in (B) were collected using a fluorescein filter set while the images in (C) were collected using a rhodamine filter set.

nanomaterial and lead to effective techniques for derivatization and washing. However, difficulties in analysing nanostructures at appropriate resolution make chemical characterization studies challenging. In general, techniques that allow for the analysis of individual structures are preferred over bulk material measurements. The ability to direct the synthesis of CNFs is helpful in this regard as individual nanofibres can be spatially addressed. The small size of nanomaterials often requires observation by SEM. However, organic coatings are difficult to observe by SEM. Further, the high vacuum environment can cause dehydration and damage to biological materials. For these reasons, fluorescence microscopy was used to assess chemical coupling to VACNFs. Fluorescence microscopy techniques are commonly used biological assays and benefit from the diverse array of reagents available and widespread acceptance of the technique. Typically, it is used as a qualitative indicator due to intrinsic and environmental effects on fluorescence intensity including dye quantum yield, quenching effects and peak wavelength shifts. Nevertheless, qualitative measures of binding can be made and the conditions used here are consistent with those typically used for biochemical assays.

### *4.1. Mechanism of adsorption specificity*

Using fluorescently labelled proteins allows for easy observation and exploits standard methods and reagents. Specifically, dyes based on rhodamine or fluorescein were used. These standard labels are easily separated spectrally and show distinct differences in their interactions with VACNFs. The rhodamine based dyes interacted strongly with the VACNFs while fluorescein did not. Rhodamine and fluorescein are structurally similar. The primary distinction is the replacement of the side-chain hydroxyls in fluorescein with amine functionalities in the rhodamine series of dyes. This difference appears to be responsible for the different binding properties. A specific coupling between the amine side-chains present in the rhodamine dyes

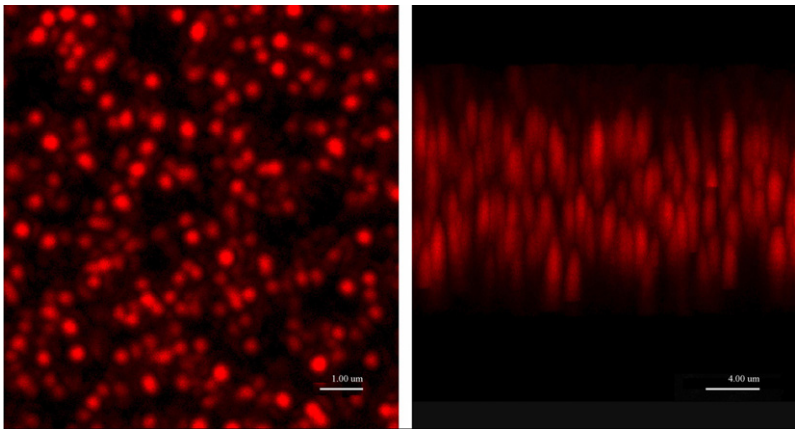


**Figure 5.** Confocal fluorescence micrographs of fluorescently labelled DNA hybridized to a complementary DNA sequence covalently tethered to a forest of carbon nanofibres. The carbon nanofibres are ∼4 $\mu$m tall. The image on the left is a view from the top while the image on the right displays a $z$-stack of images viewed at an angle. The image stack was collected across a depth of 4.2 $\mu$m with optical sections at 0.1 $\mu$m. Labelling is observed across the entire length of the nanofibres.

(This figure is in colour only in the electronic version)

with the carboxylic acid moieties on the VACNFs promotes adsorption. The washing procedures further support the importance of the amine group in the adsorption process. High ionic strength washes or high urea concentrations are needed to displace the rhodamine dyes from the carbon nanofibres while fluorescein is easily removed with distilled water.

For adsorption, the aromatic structure of the fluorescent dyes may also play a role. In the case of carbon nanotubes, the graphene outer surface allows for stacking interactions with aromatic molecules like pyrene [15, 16]. The hydrophobic outer surface is also implicated in the non-specific binding of proteins. For example, proteins such as streptavidin, bovine serum albumin and others strongly physisorb onto carbon nanotubes [22]. In the case of vertically aligned carbon nanofibres, the sidewalls also possess graphene carbon, but the sheets are present in a stacked configuration rather than the smooth outer sheathing characteristic of carbon nanotubes. In contrast to carbon nanotubes, avidin was not found to strongly physisorb to VACNFs. Further, the stacked carbon sheets lead to exposure of structural defects that can be converted to carboxylic acid moieties. This structural difference accounts for the observed differences in absorption. Although both the fluorescein and rhodamine series of dyes have the same basic aromatic structure and may allow for $\pi$-stacking interactions with exposed graphene sheets, this interaction appears negligible. Additionally, the presence of charged groups creates a more hydrophilic surface present when compared to carbon nanotubes.

Although the dye mediated binding strategy does facilitate protein immobilization using fairly gentle immobilization conditions, the reversibility of the dye binding under stringent wash conditions may preclude this strategy from some applications. Nevertheless, non-covalent adsorption is straightforward and potentially useful for diagnostic assays. Further, understanding these chemical interactions with VACNFs is important for designing wash procedures and effective assay conditions.

### *4.2. Affect of carbon nanofibre composition and preparation*

The growth conditions used to prepare the carbon nanofibres must be carefully controlled as changes in the acetylene and ammonia concentrations can affect the chemical composition of the carbon nanofibres and possibly their binding properties. While nanofibres with high carbon content are essentially non-fluorescent, growth conditions can produce nanofibres with high levels of non-carbon impurities, such as sputtered $Si_xN_y$ films. These films tend to coat the sidewall and cause the nanofibres to autofluoresce over a broad spectrum. Unfortunately, this autofluorescence prevents a detailed quantitative analysis of the chemical adsorption properties of fluorescent dyes as a function of the chemical composition of the nanofibres. Therefore, the ammonia and acetylene concentrations were adjusted to provide high carbon content nanofibres. It was observed that freshly prepared carbon nanofibres performed better in adsorption experiments than those that had aged for more than two weeks. Aged samples benefited from an oxygen plasma treatment that served to clean the surface and promote the formation of carboxylic acid sites. These treated samples then performed as well as freshly prepared samples in physisorption studies, further supporting the importance of carboxylic acid sites in promoting specific adsorption characteristics.

### *4.3. Covalent coupling*

Covalent coupling procedures present a more robust approach to immobilizing biomolecules. Standard biomolecular immobilization chemistries that exploit carbodiimide based cross-linking for immobilization to surfaces are applicable to VACNF functionalization. However, oxygen plasma cleaning appears to be necessary for effective and reproducible functionalization by this approach, supporting the assumption that carboxylic acid production results from oxygen plasma treatment. Both DNA and proteins can be immobilized by coupling pendant amine groups to the exposed carboxylic acid residues on the VACNF surface. Stringent wash conditions

could be applied and not remove the tethered biomolecules. This can be useful for removing weakly bound, physisorbed materials and for reducing background fluorescence when performing fluorescence based assays. In contrast to carbon nanotubes, functionalization appears homogeneous across the surface of VACNFs as judged by confocal fluorescence microscopy. This enables exploitation of the high surface area created by the immobilized nanostructures, allowing for higher binding capacities when compared to planar surfaces.

## 5. Conclusion

Non-covalent and covalent approaches to the chemical functionalization of carbon nanofibres have been demonstrated. A non-covalent interaction is possible through the adsorption of amine groups in certain heterocyclic aromatic compounds to VACNFs. Dyes based on rhodamine strongly adsorb while fluorescein does not. Further, it has been shown that the covalent bonding of proteins and DNA to carbon nanofibres is possible and does not adversely impact their chemical activity. These chemical interactions with carbon nanofibres are consistent with their known structure of stacked graphene sheets. The exposed ends of the sheets dictate the adsorption properties of the VACNFs, allow for functionalization through carbodiimide-based coupling, and impart greater hydrophilicity when compared to carbon nanotubes. These chemical coupling approaches combined with the ability to deterministically synthesize VACNFs will facilitate various applications in molecular assembly, chemical sensing, and cellular probing.

## Acknowledgments

We acknowledge the contributions of Kate Klein for TEM measurements and Dale Hensley for assistance with carbon nanofibre synthesis. This research was supported by NIH Grant EB000657. AVM and MLS acknowledge support from the Material Sciences and Engineering Division Program of the DOE Office of Science. A portion of this research was conducted at the Center for Nanophase Materials Sciences, which is sponsored at Oak Ridge National Laboratory by the Division of Scientific User Facilities, US Department of Energy. This work was performed at the Oak Ridge National Laboratory, managed by UT-Battelle, LLC, for the US DOE under contract No DE-AC05-00OR22725.

## References

[1] McKnight T E, Melechko A V, Austin D W, Sims T, Guillorn M A and Simpson M L 2004 *J. Phys. Chem.* B **108** 7115
[2] Lee C S, Baker S E, Marcus M S, Yang W, Eriksson M A and Hamers R J 2004 *Nano Lett.* **4** 1713
[3] McKnight T E, Melechko A V, Griffin G D, Guillorn M A, Merkulov V I, Serna F, Hensley D K, Doktycz M J, Lowndes D H and Simpson M L 2003 *Nanotechnology* **14** 551
[4] McKnight T E, Melechko A V, Hensley D K, Mann D G J, Griffen G D and Simpson M L 2004 *Nano Lett.* **4** 1213
[5] Fletcher B L, Hullander E D, Melechko A V, McKnight T E, Klein K L, Hensley D K, Simpson M L and Doktycz M J 2004 *Nano Lett.* **4** 1809
[6] Melechko A V, Merkulov V I, McKnight T E, Guillorn M A, Klein K L, Lowndes D H and Simpson M L 2005 *J. Appl. Phys.* **97** 041301
[7] Merkulov V I, Lowndes D H, Wei Y Y, Eres G and Voelkl E 2000 *Appl. Phys. Lett.* **76** 3555
[8] Ren Z F, Huang Z P, Wang D Z, Wen J G, Xu J W, Wang J H, Calvet L E, Chen J, Klemic J F and Reed M A 1999 *Appl. Phys. Lett.* **75** 1086
[9] Merkulov V I, Melechko A V, Guillorn M A, Lowndes D H and Simpson M L 2001 *Appl. Phys. Lett.* **79** 2970
[10] Sun Y-P, Kefu F, Lin Y and Huang W 2002 *Acc. Chem. Res.* **35** 1096
[11] Sinnott S B 2002 *J. Nanosci. Nanotechnol.* **2** 113
[12] Niyogi S, Hamon M A, Hu H, Zhao B, Bhowmik P, Sen M E, Itkis M E and Haddon R C 2002 *Acc. Chem. Res.* **35** 1105
[13] Dyke C A and Tour J M 2004 *J. Phys. Chem.* A **108** 11151
[14] Banerjee S, Hemraj-Benny T and Wong S S 2005 *Adv. Mater.* **17** 17
[15] Chen R J, Zhang Y, Wang D and Dai H 2001 *J. Am. Chem. Soc.* **123** 3838
[16] Chen R J, Bangsaruntip S, Drouvalakis K A, Kam N W S, Shim M, Li Y, Kim W, Utz P J and Dai H 2003 *Proc. Natl Acad. Sci. USA* **100** 4984
[17] McCarthy B, Coleman J N, Czerw R, Dalton A B, Byrne H J, Teklaeb D, Iyer P, Ajayan P M, Blau W J and Carroll D L 2001 *Nanotechnology* **12** 187
[18] Star A, Stoddart J F, Steuerman D, Diehl M, Boukai A, Wong E W, Yang X, Chung S-W, Choi H and Heath J R 2001 *Angew. Chem. Int. Edn* **40** 1721
[19] Baker S E, Tse K-Y, Hindin E, Nichols B M, Lasseter Clare T and Hamers R J 2005 *Chem. Mater.* **17** 4971
[20] Melechko A V, McKnight T E, Hensley D K, Guillorn M A, Borisevich A Y, Merkulov V I, Lowndes D H and Simpson M L 2003 *Nanotechnology* **14** 1029
[21] Merkulov V I, Guillorn M A, Lowndes D H, Simpson M L and Voelkl E 2001 *Appl. Phys. Lett.* **79** 1178
[22] Shim M, Kam N W S, Chen R J, Li Y and Dai H 2002 *Nano Lett.* **2** 285